AGU PUBLICATIONS

JGR

Journal of Geophysical Research: Space Physics

RESEARCH ARTICLE
10.1002/2016JA022382

Ion-neutral coupling effects on low-latitude thermospheric evening winds

W. Evonosky[1], A. D. Richmond[2], T.-W. Fang[3], and A. Maute[2]

[1]Department of Physics, University of South Florida, Tampa, Florida, USA, [2]HAO, National Center for Atmospheric Research, Boulder, Colorado, USA, [3]Cooperative Institute for Research in Environmental Sciences, University of Colorado Boulder, Boulder, Colorado, USA

Key Points:
- Pressure gradient, ion drag, and viscous forces are in approximate balance at low latitudes
- Ion drag approximately balances pressure gradient around EIA, supporting Rishbeth hypothesis
- Evening zonal wind shear is created by strong eastward acceleration above 200 km

Correspondence to:
A. D. Richmond,
richmond@ucar.edu

Citation:
Evonosky, W., A. D. Richmond, T.-W. Fang, and A. Maute (2016), Ion-neutral coupling effects on low-latitude thermospheric evening winds, *J. Geophys. Res. Space Physics*, *121*, 4638–4646, doi:10.1002/2016JA022382.

Received 13 JAN 2016
Accepted 18 APR 2016
Accepted article online 23 APR 2016
Published online 5 MAY 2016

Abstract We examine the forces that determine zonal wind structure in the low-latitude evening thermosphere and its relation with ion-neutral coupling. These winds drive the evening *F* region dynamo that affects the equatorial ionization anomaly (EIA) and the generation of plasma irregularities. Forces are calculated using the Thermosphere-Ionosphere-Electrodynamics General Circulation Model coupled with the Global Ionosphere-Plasmasphere model. At 19 LT, the horizontal pressure gradient dominates the net acceleration of neutral winds below ~220 km, while it tends to be offset by ion drag and viscosity higher up. The eastward pressure-gradient acceleration above 200 km increases approximately linearly with height and tends to be similar for different latitudes and different levels of solar activity. The pressure-gradient and ion-drag forces in the central *F* region approximately balance for field lines that pass through the EIA. Viscosity is an important additional force at non-EIA latitudes and in the bottomside and topside EIA ionosphere. An increase in *E* region drag on plasma convection due to increased nighttime ionization causes both the ion and neutral velocities in the *F* region to decrease, while the velocity difference tends to be maintained. The presence of a low-latitude evening time vertical shear in the zonal wind is associated primarily with a strong eastward pressure-gradient acceleration at high altitude that reverses the daytime westward wind and a weak low-altitude pressure-gradient acceleration of either eastward or westward direction that fails to reverse the low-altitude westward wind present in the afternoon.

1. Introduction

Plasma convection in the nighttime low-latitude ionosphere is strongly influenced by thermospheric winds through the *F* layer dynamo effect [*Rishbeth*, 1971a, 1971b; *Heelis et al.*, 2012; *Rodrigues et al.*, 2012; *Richmond et al.*, 2015; *Eccles et al.*, 2015]. Eastward or westward zonal winds tend to drag the plasma along, subject to the "frozen-in" constraint that all plasma particles on a geomagnetic field line essentially move together in the low-collision *F* region and to the constraint that electric current in the coupled *E* and *F* regions is divergence free. One notable phenomenon in model simulations of the low-latitude evening ionosphere is a shear in the wind from westward at low altitudes (below roughly 180 km) to eastward at high altitudes (above roughly 250 km) [*Rodrigues et al.*, 2012; *Richmond et al.*, 2015], and this is associated with a shear of plasma convection from westward on low-apex field lines to eastward on higher-apex field lines, with the transition around roughly 300 km [*Kudeki et al.*, 1981; *Tsunoda et al.*, 1981; *Fejer*, 1981; *Fejer et al.*, 1985; *Aggson et al.*, 1987; *Coley and Heelis*, 1989; *Haerendel et al.*, 1992; *Eccles et al.*, 1999; *Kudeki and Bhattacharayya*, 1999; *Mathew and Nayar*, 2011; *Lee et al.*, 2015]. Although a few observations of neutral winds above 160 km in the low-latitude evening thermosphere [*Kiene et al.*, 2015] fail to confirm the modeled wind shear, the consistency of modeled and observed plasma convection shears suggests that the modeled neutral wind shear is likely to be a common feature of the low-latitude evening winds. The longitude variation of the zonal plasma convection affects the vertical plasma drift through the condition of a curl-free electric field [*Eccles*, 1998b; *Richmond et al.*, 2015; *Eccles et al.*, 2015]. The vertical drift affects the amplitude of the equatorial ionization anomaly (EIA) and is associated with plasma instabilities that can lead to deleterious radio wave scintillations [*Anderson*, 1981; *Anderson et al.*, 2004; *Basu et al.*, 2004]. The neutral wind shear also facilitates the generation of plasma instabilities [*Hysell and Kudeki*, 2004; *Kudeki et al.*, 2007; *Woodman*, 2009]. Because the neutral winds have such a strong influence on the low-latitude evening ionosphere, it is important to understand the processes that determine these winds and their variability.

A complication of understanding the nightside winds is that not only do the winds drive the plasma convection through neutral-ion collisions but also the convection feeds back on the winds through the ion-drag effect caused by these same collisions. The ion-drag force is associated with electric currents flowing within and between the *F* and *E* regions, transferring momentum from the rarefied air in the *F* region to the much denser air in the *E* region. *Rishbeth* [1971a, 1971b, 1981] hypothesized in his theory of the *F* layer dynamo that the ion-drag force on the *F* region wind and the associated meridional electric current density of the *F* region dynamo automatically adjust to balance the horizontal pressure-gradient force on the air associated with the day-to-night pressure differences in the upper thermosphere. Since the *F* region ion-drag force is proportional to the difference between the ion and neutral velocities, Rishbeth's hypothesis implies that a change in the ion velocity should be accompanied by a corresponding change in the *F* region neutral velocity in a way that maintains an adequate ion-neutral velocity difference. As shown by *Richmond and Fang* [2015], a factor affecting the low-latitude evening *F* region ion convection velocity is the *E* region conductivity. One goal of the present paper is to determine how well the ion-neutral velocity difference is maintained when the ion velocity changes due to nighttime *E* region conductivity changes.

Rishbeth's [1971a, 1971b] concept of a balance between pressure-gradient and ion-drag forces in the *F* region has been used in numerical models of the electric fields generated by the *F* layer dynamo [*Rishbeth*, 1971b; *Matuura*, 1974], under the implicit assumption that the horizontal pressure gradient does not itself respond to changes of the wind. In reality the pressure gradient is not independent of the wind but is dynamically connected to it [e.g., *Dickinson et al.*, 1971]. Divergent/convergent winds tend to reduce horizontal pressure gradients, with the changes essentially being transmitted via gravity waves at horizontal speeds up to the limiting gravity wave speed, approximately 800 m/s in the upper thermosphere, depending on temperature and background winds. Smaller-scale horizontal pressure gradients can be suppressed more quickly than larger-scale pressure gradients. However, the rate at which horizontal pressure gradients can be reduced is slowed by gravity-wave dissipation associated with ion drag, viscosity, and heat conduction in the thermosphere. It is for this reason that a large night-to-day pressure gradient can be maintained in the upper thermosphere in spite of the fact that the daily westward migration of solar heating is slower (about 480 m/s at the equator) than the limiting gravity-wave speed in the upper thermosphere. A second goal of this paper is to quantify how well horizontal pressure gradients can be maintained in the presence of spatially varying winds and ion drag in the low-latitude evening thermosphere.

Richmond et al. [2015] suggested that the low-latitude evening zonal wind shear could be caused by the change from weak ion drag at low altitudes to strong ion drag at higher altitudes, owing to the strong variations of ion density with height at night. They noted that where ion drag is strong, the ion-drag force tends to balance the eastward horizontal pressure-gradient force existing in the evening, resulting in an eastward wind. At lower altitudes, where ion drag is weak, they proposed that the eastward horizontal pressure gradient in the evening would not be balanced by ion drag but rather by wind acceleration, leading to a retardation of the transition from daytime westward winds to nighttime eastward winds, so that the wind could remain westward into the evening. The different responses of the wind to the pressure gradient at low and high altitudes could then produce a wind shear like that observed in model simulations. A third goal of this paper is to test whether the proposed mechanism of *Richmond et al.* [2015] for creating the neutral wind shear is supported by model simulations.

2. Method

Our analysis of forces on the air in the low-latitude evening thermosphere uses the simulations carried out by *Richmond et al.* [2015] and *Richmond and Fang* [2015] with the NCAR Thermosphere-Ionosphere-Electrodynamics General Circulation Model (TIEGCM) [*Qian et al.*, 2013], two-way coupled with the Global Ionosphere-Plasmasphere (GIP) model [*Fang et al.*, 2009]. The TIEGCM is run on a 5° × 5° longitude-latitude grid, with 0.5 scale height vertical resolution. The TIEGCM neutral parameters are interpolated to the GIP magnetic-coordinate grid, with 4.5° longitude spacing and variable spacing in magnetic latitude and along field lines. The GIP model calculates ion and electron densities, which are used together with the neutral densities and velocities to calculate conductivities and wind-driven current densities that are utilized by the TIEGCM to solve for the electric potential. The electric fields and the GIP ion densities are then interpolated to the TIEGCM geographic grid to calculate the neutral dynamics. The TIEGCM lower boundary is forced by migrating atmospheric tidal climatology from *Hagan and Forbes* [2002, 2003]. Since the focus of this study is

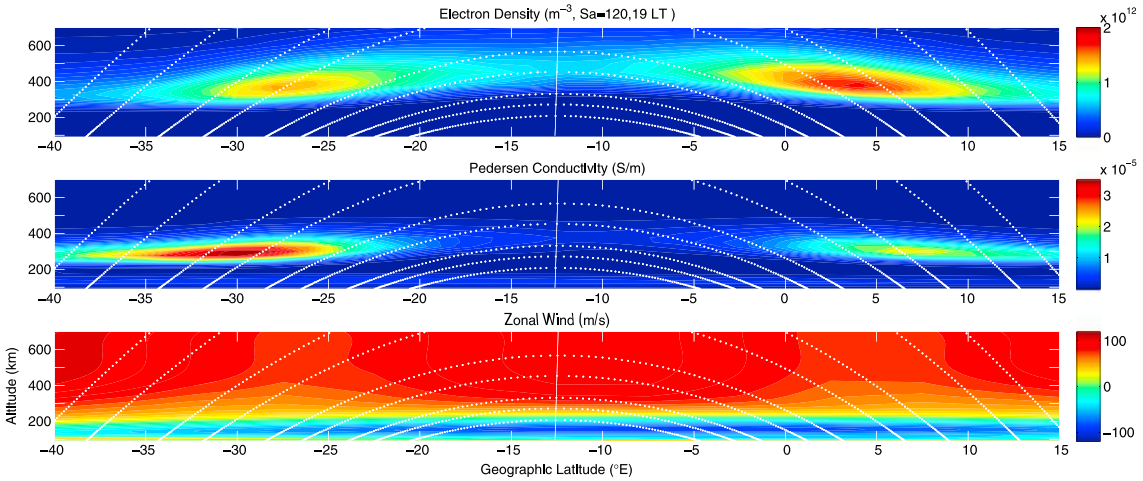

Figure 1. Low-latitude electron density, Pedersen conductivity and eastward wind for the base case simulation (see text) at 75°W longitude, 0 UT (19 LT), with equal scales for latitudinal distance and height. Dotted lines are geomagnetic field lines. The nearly vertical lines around −12.5° latitude trace the magnetic equator with altitude. From *Richmond et al.* [2015].

on low latitudes, magnetospheric influences are neglected by setting the electric potential to nearly zero at 60° magnetic latitude. All simulations are for March equinox.

The base case is for moderate solar activity (solar 10.7 cm radio flux index $S_a = 120$) and uses the standard TIEGCM nighttime ionization rate described by *Richmond and Maute* [2013]. Two more simulations are for low ($S_a = 70$) and high ($S_a = 200$) solar activity with the standard nighttime ionization. The final two simulations are for moderate solar activity ($S_a = 120$) but with the nighttime ionization rate either decreased or increased by a factor of 10, which reduces or increases the *E* region conductivities by a factor of about 3.2. As discussed by *Richmond and Fang* [2015], there is considerable uncertainty and variability of the nighttime ionization rate and *E* region conductivity, which affects the nighttime electrodynamics. The standard TIEGCM nighttime ionization rate results in electric fields that are generally compatible with observations, which themselves are quite variable. However, the TIEGCM neglects the redistribution of nighttime *E* region plasma by electric fields and neutral winds, owing to its assumption that molecular ions are in photochemical equilibrium, and it also neglects the presence of metallic ions. The simple increase or decrease of nighttime *E* region electron densities by a factor of 3.2 may adequately reflect the actual variability at a given height but probably overestimates the variability of the height-integrated conductivities. Nevertheless, these simulations help us to understand the importance of nighttime *E* region conductivities on the *F* region neutral and ion dynamics.

Figure 1, from *Richmond et al.* [2015], shows features of the low-latitude ionosphere for the base case at 75°W longitude, at 19 local time (0 UT). At this longitude the magnetic declination is small, and the displayed plane is nearly a magnetic meridian. As noted by *Richmond et al.* [2015], the Pedersen conductivity (Figure 1, middle) maximizes in the lower *F* region at the base of the EIA in both the southern and northern magnetic hemispheres. The *F* region Pedersen conductivity is proportional not only to the ion density but also to the neutral density and the inverse square of the magnetic field strength. The facts that the *F* layer is slightly lower in the Southern Hemisphere than in the north and that the Southern Hemisphere at this longitude has a weaker magnetic field because of the South Atlantic Anomaly result in a stronger Pedersen conductivity in the south, even though the southern EIA electron density peak is weaker than the northern peak. The regions of largest Pedersen conductivity are where frictional coupling between the neutrals and the ions is greatest and where winds most strongly influence evening equatorial electrodynamics. The present study focuses on two features of the neutral zonal wind (Figure 1, bottom): a strong shear in altitude, maximizing around 200 km altitude; and a moderate variation in latitude in the upper thermosphere, with relative minima in the EIA regions.

The tendency equation for the eastward velocity can be written as

$$\frac{\partial u}{\partial t} + \frac{u}{R\cos\lambda}\frac{\partial u}{\partial \phi} + \frac{v}{R}\frac{\partial u}{\partial \lambda} + w\frac{\partial u}{\partial z} - fv = \frac{-1}{R\cos\lambda}\frac{\partial \Phi}{\partial \phi} - \nu_{ni}(u - u_i) + \frac{1}{\rho}\frac{\partial}{\partial z}\left(\mu\frac{\partial u}{\partial z}\right) \quad (1)$$

where t, ϕ, λ, and z are time, longitude, latitude, and altitude, respectively; R is the Earth radius plus altitude; u, v, and w are the geographic eastward, northward, and vertical velocities; f is the Coriolis parameter, Φ is the

gravitational geopotential, u_i is the geographic eastward ion velocity, ν_{ni} is the neutral-ion collision frequency (proportional to the ion density), ρ is total mass density, and μ is the coefficient of molecular viscosity. Pressure coordinates are used, such that horizontal partial derivatives are calculated at constant pressure rather than constant altitude. For the conditions under consideration the nonlinear momentum-advection terms (the second, third, and fourth terms on the left-hand side) are much smaller than the other terms, so we neglect them in our analysis (although they are included in the model simulations). We also find that the zonal Coriolis acceleration (the last term on the left-hand side) is negligible at the low latitudes examined, because either f or v, or both, is small. We therefore focus on the neutral wind tendency $\partial u/\partial t$ and on the terms on the right-hand side: pressure-gradient acceleration, ion drag, and viscous acceleration.

The ion-drag acceleration can also be expressed in terms of the difference between the neutral velocity and the $\mathbf{E} \times \mathbf{B}/B^2$ electrodynamic convection velocity, where **E** and **B** are the electric and magnetic fields. This electrodynamic convection velocity is usually called the "E-cross-B" ($E \times B$) velocity. In the F region the ion velocity perpendicular to **B** nearly equals the $E \times B$ velocity, but more frequent ion-neutral collisions below 150 km cause the two velocities to differ in the E region. When the $E \times B$ velocity is used instead of u_i for calculating ion drag, the multiplying coefficient of the velocity difference also departs from ν_{ni} in the E region, where the coefficient becomes a tensor. Since the influence of neutral-ion collisions on neutral dynamics in the nighttime E region is very small, we concentrate here only on their importance for neutral dynamics in the nighttime F region, where it is justified to refer to the $E \times B$ velocity as the ion velocity perpendicular to **B**.

3. Results

We find that the eastward pressure-gradient force in the upper thermosphere maximizes around 19 LT, and so we focus on this local time to see how the forces are affecting the wind. The model results are similar at different longitudes, and results are shown only at 75° W geographic longitude, as in Figure 1. At this longitude the magnetic equator lies at approximately −12.5° geographic latitude, and the northern EIA crest lies near 2.5° geographic latitude (approximately 15° magnetic latitude). The southern EIA crest lies sufficiently far from the geographic equator that Coriolis effects are no longer entirely negligible, so we focus in this study on the northern crest and the magnetic equator.

Figure 2 shows vertical profiles of various velocities and acceleration terms acting on the air at the magnetic equator and at 15° north magnetic latitude for our base case. At both latitudes the eastward neutral wind (Figure 2, middle, blue lines) has similar values below about 300 km, becoming westward below 225 km. Above 300 km the wind is more strongly eastward at the magnetic equator than at 15° magnetic latitude, as also seen in Figure 1. The red lines in Figure 2 (middle) show the zonal $E \times B$ velocities above 150 km. At these altitudes the ions drift at nearly the $E \times B$ velocity, and so the curves are labeled "Ion Velocity." The ion velocities are quite different at the two locations: at the magnetic equator they are westward below 375 km, but at 15° magnetic latitude they are approximately 30 m/s eastward at all altitudes. The eastward ion velocity is determined for each geomagnetic field line primarily by the field line-averaged conductivity and conductivity-weighted winds on that field line [*Rishbeth*, 1971b; *Haerendel et al.*, 1992; *Rodrigues et al.*, 2012; *Richmond et al.*, 2015; *Eccles et al.*, 2015]. At the equator, a large number of field lines with varying averaged winds and conductivities are traversed from the bottom to the top of the ionosphere, while at higher latitudes far fewer field lines are traversed, accounting for the much smaller altitude variation of ion velocity there. In Figure 2 (right) are the ion-drag coefficients at the two locations, essentially equal to the neutral-ion collision frequencies above 150 km. The F region ion-drag coefficient is proportional to the ion density and is much larger at 15° magnetic latitude than at the magnetic equator at this time.

The eastward pressure-gradient acceleration in Figure 2 (left, black lines) grows almost linearly with height above about 200 km and is remarkably similar at the two latitudes. One might think that the latitude variation of the eastward neutral wind above 300 km would be associated with a similar latitude variation of the zonal pressure gradient, owing to dynamical feedback of winds on the pressure, but Figure 2 shows that the percentage variation of the zonal pressure-gradient acceleration with respect to latitude is considerably less than that of the zonal wind. What keeps the pressure and its evening time westward gradient relatively uniform in latitude is the fact that pressure nonuniformities tend to be dynamically smoothed out through convergent/divergent winds, as described in section 1. The timescale for smoothing in the north-south direction is on the order of the horizontal size of the disturbance (~1600 km for the distance from the magnetic equator to an EIA crest) divided by the limiting gravity-wave speed, on the order of 0.8 km/s in the upper thermosphere,

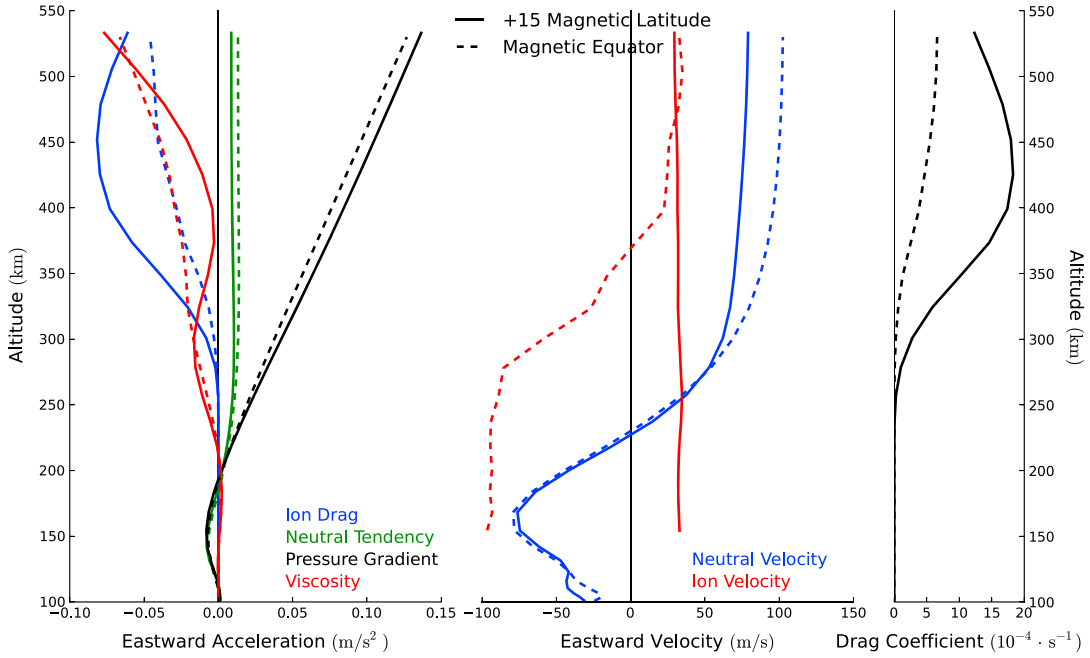

Figure 2. (left) Eastward acceleration terms, (middle) eastward neutral and $E \times B$ ("Ion") velocities, and (right) ion-drag coefficient vertical profiles all with the same height scale, for our base case, at 75°W geographic longitude, 0 UT (19 LT), for two latitudes. The solid and dashed lines are for +2.5° and −12.5° geographic latitude (+15° and 0° magnetic latitude), respectively.

giving a pressure-smoothing timescale on the order of 2000 s (33 min). This timescale is supported by simulations of *Hsu et al.* [2014], who analyzed the establishment of meridional winds associated with field-aligned ion-drag forces at low latitudes. In contrast, the scale size of the pressure gradient in the zonal direction is much larger, and it relaxes on a correspondingly longer timescale, comparable with the westward propagation time of this feature at the speed of the terminator. The zonal pressure gradients are therefore generated as fast as they are diluted by convergent/divergent winds. Also contributing to the more rapid reduction of meridional than zonal pressure gradients is the fact that winds in the meridional direction are much less affected by ion drag than are winds in the zonal direction, owing to the nearly horizontal meridionally aligned geomagnetic field lines near the magnetic equator.

The eastward neutral wind tendency in Figure 2 (left, green lines), which is nearly the same as the net eastward acceleration, approximately equals the pressure-gradient acceleration below 210 km at both locations but then asymptotes to around 0.01 m/s^2 above 250 km, while the pressure-gradient acceleration continues to grow with height. The difference between the net acceleration and the pressure-gradient acceleration essentially matches the sum of the ion-drag (blue lines) and viscous (red lines) accelerations. Although this sum is similar at the two latitudes, the height variations of ion drag and viscosity are quite different. Ion drag is weaker at the magnetic equator, where viscosity is the main force offsetting the pressure-gradient force. At 15° magnetic latitude, on the other hand, ion drag is larger than viscosity between 310 and 530 km, although viscosity remains the primary drag force on the wind below 310 km and above 530 km. Below 300 km at both latitudes ion drag is small, and only viscosity can provide enough drag to help balance the pressure-gradient acceleration when the latter grows larger than the wind tendency. This viscous acceleration is associated with a strong vertical curvature (second derivative with height) of the neutral velocity, seen in Figure 2 (middle).

Based on results for geographic latitudes between about ±30°, the following picture emerges. The eastward horizontal pressure-gradient acceleration is fairly uniform in latitude and increases approximately linearly with altitude above 200 km, greatly exceeding the net acceleration or wind tendency above 250 km. Offsetting this excess pressure-gradient acceleration is the sum of ion-drag and viscous accelerations, the relative fractions of which vary greatly both with latitude and height. The fact that ion drag is often the dominant force opposing the pressure-gradient force supports the hypothesis of *Rishbeth* [1971a, 1971b] concerning the evening *F* layer dynamo. The facts that viscosity often plays a comparable role with ion drag and that net acceleration is not negligible below 250 km in comparison with these other acceleration terms require a modification of

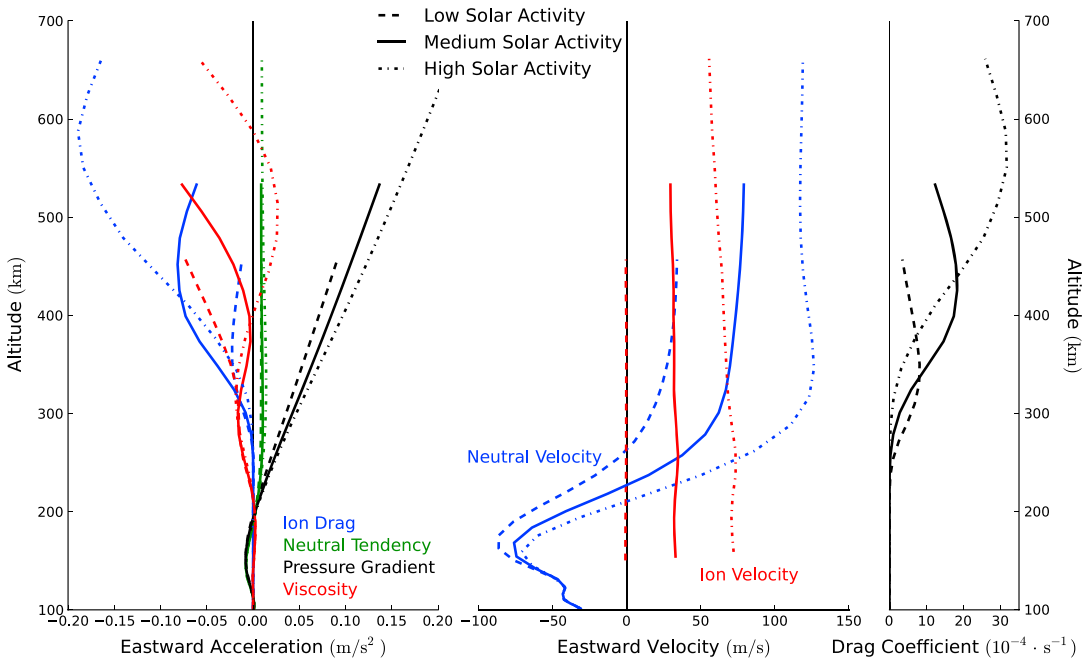

Figure 3. (left) Eastward acceleration terms, (middle) eastward neutral and $E \times B$ (Ion) velocities, and (right) ion-drag coefficients at 2.5° geographic latitude (15° magnetic latitude), 75° W geographic longitude, 0 UT (19 LT), for different levels of solar activity. The solid lines are our base case of medium solar activity ($S_a = 120$); dashed lines are for low activity ($S_a = 70$); and dash-dotted lines are for high activity ($S_a = 200$).

Rishbeth's hypothesis. The fact that the pressure-gradient acceleration and the net eastward acceleration are small or negative below 200 km at 19 LT is contrary to the hypothesis of *Richmond et al.* [2015], who supposed that the wind is being accelerated from westward to eastward by an eastward pressure-gradient force at this time. Therefore, the explanation proposed by *Richmond et al.* [2015] for the strong early-evening vertical shear of the zonal wind is not valid. Instead, the wind shear at this time is due to the strong high-altitude eastward acceleration by the horizontal pressure gradient in the late afternoon, and to the lack of a strong low-altitude eastward acceleration. Viscosity acts to reduce the shear. Atmospheric tides propagating up from the lower atmosphere also modulate the low-altitude (160 km) zonal wind, as can be seen in Figure 2 of *Richmond et al.* [2015]. That figure indicates an equatorial semidiurnal tidal amplitude of about 50 m/s at 160 km, directed westward at 19 LT. The tide therefore increases the wind shear at this time. However, the wind shear would be present even without the tide.

Figure 3 shows the velocities and forcing terms at 15° magnetic latitude for different levels of solar activity. There are large variations of the ion-drag coefficient (Figure 3 ,right): both the peak value and the altitude of the peak increase with solar activity. The neutral wind velocity (Figure 3 ,middle, blue lines) is increasingly eastward (or decreasingly westward) with increasing activity, and high-altitude winds are much stronger at solar maximum than minimum. The altitude of maximum wind shear, however, is similar for all three cases, around 220 km. The increase of the *F* region wind with solar activity is connected with a strong increase of ion velocity (Figure 3, middle, red lines). The horizontal pressure-gradient acceleration (Figure 3, left, black lines) and the wind tendency (green lines) show surprisingly modest variations with solar activity. Up to about 320 km the viscous acceleration (red lines) is very similar among the three cases and has a larger amplitude than the ion drag acceleration (blue lines) but varies strongly among the cases above that height. The amplitude of ion drag exceeds that of viscosity above 340 km for $S_a = 200$ and above 320 km for $S_a = 120$ but is smaller than viscosity at almost all altitudes for $S_a = 70$. When viscosity is important, we would not expect the hypothesis of *Rishbeth* [1971a, 1971b] concerning a rough force balance between pressure gradient and ion drag to be valid.

The simulations with different nighttime ionization rates give us an opportunity to see how the *F* region wind and ion-drag acceleration respond to changes in the ion velocity. As described by *Richmond and Fang* [2015], an increase in the nighttime ionization affects ion velocities through both the Pedersen and Hall conductivities in the *E* region. An increased *E* region Pedersen conductivity increases the *E* region drag on the eastward

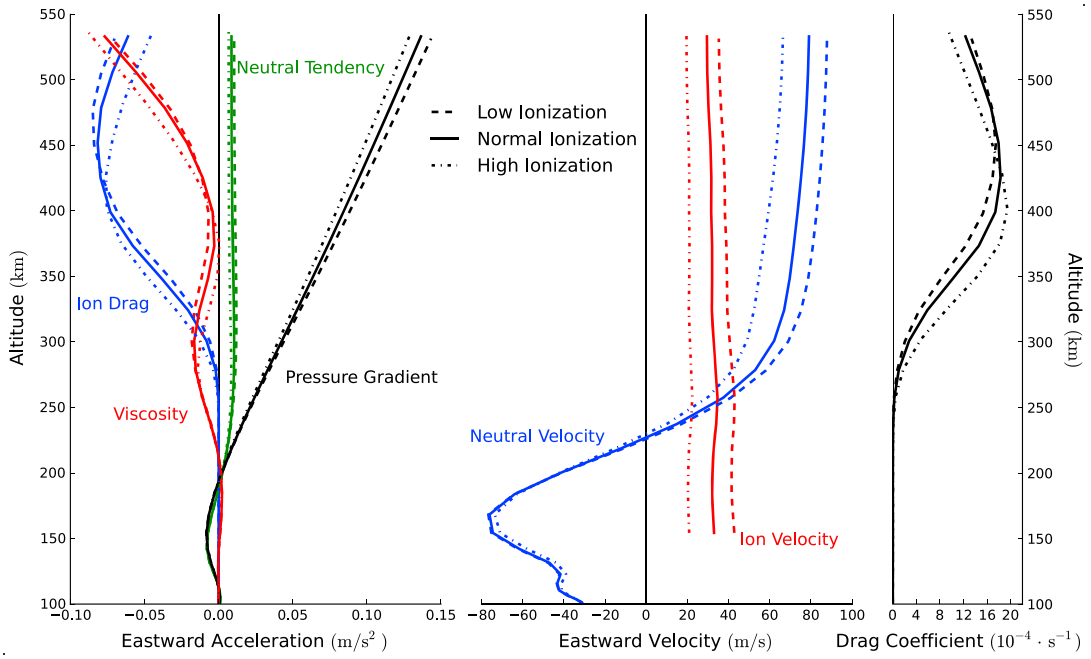

Figure 4. (left) Eastward acceleration terms, (middle) eastward neutral and $E \times B$ (Ion) velocities, and (right) ion-drag coefficients at 2.5° geographic latitude (15° magnetic latitude), 75° W geographic longitude, 0 UT (19 LT), for different levels of nighttime ionization. The solid lines are our base case and the dashed and dash-dotted lines are for lower and higher nighttime ionization, respectively (see text).

ion convection along the entire field line, slowing the eastward ion velocity in both the *E* and *F* regions. An increased *E* region Hall conductivity increases the drag on the vertical convection velocity through the *E* region Cowling conductance, which indirectly slows the eastward *F* region convection velocity as well, owing to the requirement for flow continuity (curl-free electric field). A reduction in nighttime ionization has the opposite effect, leading to an increase in the eastward *F* region ion velocity.

Richmond and Fang's [2015] description of how the ion convection velocity responds to conductivity changes was based on a specified distribution of neutral wind, but the wind itself responds to changes in the ion velocity. According to *Rishbeth*'s [1971a, 1971b] hypothesis, the wind should respond in a way to maintain the ion-drag deceleration needed to balance the pressure-gradient acceleration. If the ion-drag coefficient does not change much, then the eastward neutral wind must change in such a way so as to maintain the required neutral-ion velocity difference. This effect should be clearest under conditions where the ion-drag force dominates over viscous drag, meaning at locations of large ion density, especially the EIA region for moderate to high solar activity.

Figure 4 largely substantiates this concept. Because the simulations were run until a steady (diurnally reproducible) state was reached, the ion density and ion-drag coefficient (Figure 4, right) differ for the three simulations, owing to different strengths of the prereversal enhancement of vertical drift. The changes of nighttime *E*-region ionization have a substantial effect on both the ion velocity (Figure 4, middle, red lines) and the neutral velocity (Figure 4, middle, blue lines) above 250 km. In contrast, the changes of the acceleration terms (Figure 4, left) are much less. The wind tendency (green lines) remains small for all three cases, and the pressure-gradient acceleration (black lines) varies only slightly. The ion-drag (blue lines) and viscous (red lines) accelerations vary somewhat more but fractionally much less than the wind and ion velocities at most heights. The variations of the ion-drag and viscous accelerations that do occur are in opposite directions at almost all heights, and these variations tend to cancel when the two accelerations are summed. Above 330 km ion drag is the dominant drag force that tends to offset the pressure-gradient force, and its variations among the three cases have height profiles quite similar to the corresponding height profiles of the ion-drag coefficient. The differences between the neutral and ion velocities, which also factor into the ion-drag acceleration, are similar for the three cases. That is, the neutral and ion velocities tend to adjust together to preserve the velocity difference needed to maintain the ion-drag force which largely offsets the pressure-gradient force at these heights, as predicted by *Rishbeth*'s [1971a, 1971b] hypothesis. However, as noted above, in the 250–300 km height

range it is no longer ion drag but rather viscosity that is the main force offsetting the pressure-gradient force. Therefore, Rishbeth's hypothesis tends to overestimate the ion-drag force on the wind. Since the ion-drag force corresponds to electric current flowing perpendicular to the magnetic field, Rishbeth's hypothesis overestimates the current, the electric field, and the plasma convection associated with the *F* layer dynamo. The overestimation is particularly problematic for low solar activity and for altitudes where viscous drag exceeds ion drag.

4. Conclusions

Our analysis of forces on the air in the low-latitude evening thermosphere helps to clarify how varying ionospheric conditions affect the zonal wind and its shear, which in turn drive the zonal and vertical plasma drifts that redistribute the plasma and affect the generation of plasma irregularities. Our main findings are as follows.

In the upper low-latitude evening thermosphere there exists an approximate force balance among the eastward pressure-gradient force, the ion-drag force, and the viscous force. The eastward pressure-gradient acceleration at 19 LT above 200 km increases approximately linearly with height and tends to be similar for different latitudes (between $\pm 30°$) and for different levels of solar activity. Below 200 km the pressure gradient, while small, tends to dominate over ion drag and viscosity and drives a net acceleration of the air.

The eastward high-altitude evening pressure-gradient acceleration around 19 LT varies much less in latitude than the eastward wind velocity or ion-drag and viscous accelerations, apparently because the time for meridionally propagating gravity waves to reduce north-south pressure variations over this latitude range is short in comparison with the timescale for variations of the neutral wind and its acceleration. This insensitivity of the pressure gradient to the latitude structure of the zonal wind helps justify simplified modeling of the winds and electrodynamics under the assumption of a prespecified pressure distribution, as done, for example, by *Rishbeth* [1971b], *Heelis et al.* [1974], and *Matuura* [1974].

Rishbeth's [1971a, 1971b] hypothesis of a balance between the pressure-gradient and ion-drag forces in the *F* region is often, but not always, a good way to estimate the *F* region meridional current density for field lines that pass through the EIA region. Its validity in the evening is poor for low solar activity, when *F* region ion drag is usually weaker than viscosity. Its validity in the evening is also poor at the magnetic equator, for all levels of solar activity. Even at the EIA for moderate solar activity viscous drag becomes important in comparison with ion drag below and above the *F* peak.

A consequence of Rishbeth's hypothesis is that changes in *F* region ion velocity due to changes in *E* region conductivity are predicted to be accompanied by similar changes of *F* region neutral velocity, so that the ion-drag force on the wind continues to approximately balance the pressure-gradient force. Our simulations with altered nighttime *E* region conductivity, for moderate solar activity, are generally consistent with this prediction around the EIA crest.

The presence of a low-latitude evening time vertical shear in the zonal wind is associated primarily with a strong eastward pressure-gradient acceleration at high altitude that reverses the daytime westward wind and a weak low-altitude pressure-gradient acceleration of either eastward or westward direction that fails to reverse the low-altitude westward wind present in the afternoon. This result disproves the hypothesis of *Richmond et al.* [2015], who incorrectly assumed that the pressure-gradient acceleration was eastward at all heights concerned and proposed that the low-altitude westward wind represented merely a delayed response of the afternoon wind to this acceleration, due to inertia of the air.

Acknowledgments
Simulation outputs used in this study are archived on the NCAR Yellowstone computer system and can be obtained upon request from Tzu-Wei Fang (Tzu-Wei.Fang@noaa.gov). We thank Gang Lu for helpful comments. W.E. was supported through the Significant Opportunities in Atmospheric Research and Science (SOARS) program. W.E., A.R., and A.M. were supported in part by NSF grant AGS-1135446. T.W.F. was supported in part by NSF grant AGS-1138784. The National Center for Atmospheric Research is sponsored by the National Science Foundation.

References

Aggson, T. L., N. C. Maynard, F. A. Herrero, H. G. Mayr, L. H. Brace, and M. C. Liebrecht (1987), Geomagnetic equatorial anomaly in zonal plasma flow, *J. Geophys. Res.*, *92*, 311–315.

Anderson, D. N. (1981), Modeling the ambient, low latitude F region ionosphere—A review, *J. Atmos. Terr. Phys.*, *43*, 753–762.

Anderson, D. N., B. Reinisch, C. Valladares, J. Chau, and O. Veliz (2004), Forecasting the occurrence of ionospheric scintillation activity in the equatorial ionosphere on a day-to-day basis, *J. Atmos. Sol. Terr. Phys.*, *66*, 1567–1572.

Basu, B., J. M. Retterer, O. de La Beaujardière, C. E. Valladares, and E. Kudeki (2004), Theoretical relationship between maximum value of the post-sunset drift velocity and peak-to-valley ratio of anomaly TEC, *Geophys. Res. Lett.*, *31*, L03807, doi:10.1029/2003GL018725.

Coley, W. R., and R. A. Heelis (1989), Low-latitude zonal and vertical ion drifts seen by DE 2, *J. Geophys. Res.*, *89*, 6751–6761.

Dickinson, R. E., R. G. Roble, and E. C. Ridley (1971), Response of the neutral thermosphere at F-layer heights to interaction of a global wind with anomalies of ionization, *J. Atmos. Sci.*, *28*, 1280–1293.

Eccles, J. V. (1998b), Modeling investigation of the evening prereversal enhancement of the zonal electric field in the equatorial ionosphere, *J. Geophys. Res.*, *103*, 26,709–26,719.

Eccles, J. V., N. Maynard, and G. Wilson (1999), Study of the evening plasma drift vortex in the low-latitude ionosphere using San Marco electric field measurements, *J. Geophys. Res.*, *104*, 28,133–28,143.
Eccles, J. V., J. P. St. Maurice, and R. W. Schunk (2015), Mechanisms underlying the prereversal enhancement of the vertical plasma drift in the low-latitude ionosphere, *J. Geophys. Res. Space Physics*, *120*, 4950–4970, doi:10.1002/2014JA020664.
Fang, T.-W., H. Kil, G. Millward, A. D. Richmond, J.-Y. Liu, and S.-J. Oh (2009), Causal link of the wave-4 structures in plasma density and vertical plasma drift in the low-latitude ionosphere, *J. Geophys. Res.*, *114*, A10315, doi:10.1029/2009JA014460.
Fejer, B. G. (1981), The equatorial ionospheric electric fields. A review, *J. Atmos. Terr. Phys.*, *53*, 377–383.
Fejer, B. G., E. Kudeki, and D. T. Farley (1985), Equatorial F region zonal plasma drifts, *J. Geophys. Res.*, *90*, 12,249–12,255.
Haerendel, G., J. V. Eccles, and S. Çakir (1992), Theory for modeling the equatorial evening ionosphere and the origin of the shear in the horizontal plasma flow, *J. Geophys. Res.*, *97*(A2), 1209–1223, doi:10.1029/91JA02226.
Hagan, M. E., and J. M. Forbes (2002), Migrating and nonmigrating diurnal tides in the middle and upper atmosphere excited by tropospheric latent heat release, *J. Geophys. Res.*, *107*(D24), 4754, doi:10.1029/2001JD001236.
Hagan, M. E., and J. M. Forbes (2003), Migrating and nonmigrating semidiurnal tides in the upper atmosphere excited by tropospheric latent heat release, *J. Geophys. Res.*, *108*(A2), 1062, doi:10.1029/2002JA009466.
Heelis, R. A., P. C. Kendall, R. J. Moffett, D. W. Windle, and H. Rishbeth (1974), Electrical coupling of the *E*- and *F*-regions and its effect of *F*-region drifts and winds, *Planet. Space Sci.*, *22*, 743–756.
Heelis, R. A., G. Crowley, F. Rodrigues, A. Reynolds, R. Wilder, I. Azeem, and A. Maute (2012), The role of zonal winds in the production of a pre-reversal enhancement in the vertical ion drift in the low latitude ionosphere, *J. Geophys. Res.*, *117*, A08308, doi:10.1029/2012JA017547.
Hsu, V. W., J. P. Thayer, J. Lei, and W. Wang (2014), Formation of the equatorial thermosphere anomaly trough: Local time and solar cycle variations, *J. Geophys. Res. Space Physics*, *119*, 10,456–10,473, doi:10.1002/2014JA020416.
Hysell, D. L., and E. Kudeki (2004), Collisional shear instability in the equatorial F region ionosphere, *J. Geophys. Res.*, *109*, A11301, doi:10.1029/2004JA010636.
Kiene, A., M. F. Larsen, and E. Kudeki (2015), Equatorial F-region neutral winds and shears near sunset measured with chemical release techniques, *J. Geophys. Res. Space Phys.*, *120*, 9004–9013, doi:10.1002/2015JA021462.
Kudeki, E., and S. Bhattacharayya (1999), Postsunset vortex in equatorial *F*-region plasma drifts and implications for bottomside spread-*F*, *J. Geophys. Res.*, *104*, 28,163–28,170.
Kudeki, E., B. G. Fejer, D. T. Farley, and H. M. Ierkic (1981), Interferometer studies of equatorial F region irregularities and drifts, *Geophys. Res. Lett.*, *8*, 377–380.
Kudeki, E., A. Akgiray, M. A. Milla, J. L. Chau, and D. L. Hysell (2007), Equatorial spread-F initiation: Post-sunset vortex, thermospheric winds, gravity waves, *J. Atmos. Sol. Terr. Phys.*, *69*, 2416–2427.
Lee, W. K., H. Kil, Y.-S. Kwak, and L. J. Paxton (2015), Morphology of the postsunset vortex in the equatorial ionospheric plasma drift, *Geophys. Res. Lett.*, *42*, 9–14, doi:10.1002/2014GL062019.
Mathew, T. J., and S. R. P. Nayar (2011), Vertical shear at the equatorial F-region ionosphere during post-sunset hours, *Adv. Space Res.*, *49*, 1277–1281, doi:10.1016/j.asr.2012.01.011.
Matuura, N. (1974), Electric fields deduced from the thermospheric model, *J. Geophys. Res.*, *79*, 4679–4689.
Qian, L., A. G. Burns, B. A. Emery, B. Foster, G. Lu, A. Maute, A. D. Richmond, R. G. Roble, S. C. Solomon, and W. Wang (2013), The NCAR TIE-GCM: A community model of the coupled thermosphere/ionosphere system, in *Modeling the Ionosphere-Thermosphere System, Geophys. Monogr.*, vol. 201, edited by J. Huba, R. Schunk, and G. Khazanov, pp. 73–83, AGU, Washington, D. C., (also published online in 2014 by John Wiley, Chichester, U. K., doi:10.1002/9781118704417.ch7), doi:10.1029/2012GM001297.
Richmond, A. D., and T.-W. Fang (2015), Electrodynamics of the equatorial evening ionosphere: 2. Conductivity influences on convection, current, and electrodynamic energy flow, *J. Geophys. Res. Space Phys.*, *120*, 2133–2147, doi:10.1002/2014JA020935.
Richmond, A. D., and A. Maute (2013), Ionospheric electrodynamics modeling, in *Modeling the Ionosphere-Thermosphere System, Geophys. Monogr.*, 201, edited by J. Huba, R. Schunk, and G. Khazanov, pp. 57–71., (also published online in 2014 by John Wiley and Sons, Ltd, Chichester, U. K., doi:10.1002/9781118704417.ch6), doi:10.1029/2012GM001331.
Richmond, A. D., T.-W. Fang, and A. Maute (2015), Electrodynamics of the evening equatorial ionosphere—I. Importance of winds in different regions, *J. Geophys. Res.*, *120*, 2118–2132, doi:10.1002/2014JA020934.
Rishbeth, H. (1971a), The *F*-layer dynamo, *Planet. Space Sci.*, *19*, 263–267.
Rishbeth, H. (1971b), Polarization fields produced by winds in the equatorial *F*-region, *Planet. Space Sci.*, *19*, 357–369.
Rishbeth, H. (1981), The F-region dynamo, *J. Atmos. Terr. Phys.*, *43*, 387–392.
Rodrigues, F. S., G. Crowley, R. A. Heelis, A. Maute, and A. Reynolds (2012), On TIE-GCM simulation of the evening equatorial plasma vortex, *J. Geophys. Res.*, *117*, A05307, doi:10.1029/2011JA017369.
Tsunoda, R. T., R. C. Livingston, and C. L. Rino (1981), Evidence of a velocity shear in bulk plasma motion associated with the post-sunset rise of the equatorial F-layer, *Geophys. Res. Lett.*, *8*, 807–810.
Woodman, R. F. (2009), Spread F—An old equatorial aeronomy problem finally resolved?, *Ann. Geophys.*, *27*, 1915–1934.